Atmos. Meas. Tech. Discuss., https://doi.org/10.5194/amt-2018-385
Manuscript under review for journal Atmos. Meas. Tech.
Discussion started: 15 November 2018

Atmospheric Measurement Techniques Discussions

High−precision measurements of nitrous oxide and methane in air with cavity ring-down spectroscopy at 7.6μm

Jing Tang, Bincheng Li, Jing Wang

School of Optoelectronic Science and Engineering, University of Electronic Science and Technology of China, Chengdu 610054, China

Correspondence to: Bincheng Li (bcli@uestc.edu.cn)

Abstract. A high-sensitivity methane (CH_4) and nitrous oxide (N_2O) sensor based on mid-infrared continuous-wave (cw) cavity ring-down spectroscopy (CRDS) technique was developed for environmental and biomedical trace gas measurements. A tunable external-cavity mode-hop-free (EC-MHF) quantum cascade laser (QCL) operating at 7.4 to 7.8 μm was used as the light source. The effect of temperature fluctuation on the measurement sensitivity of the CRDS experimental setup was analyzed and corrected, and a sensitivity limit of absorption coefficient measurement of 7.38×10^{-10} cm^{-1} was achieved at 1330.50 cm^{-1} with an average of 176 measurements, or 26.4-seconds averaging time, and further improved to 1.70×10^{-10} cm^{-1} with average of 3266 measurements, or 490-seconds averaging time. For the targeted CH_4 and N_2O absorption lines located at 1298.60 cm^{-1} and 1327.07 cm^{-1}, with temperature effect correction detection limits of 18.2 pptv and 14.9 pptv were experimentally achieved with 24.9-seconds and 20.5-seconds averaging time, and could be further improved to 3.62 pptv and 4.67 pptv with 513-seconds and 461-seconds averaging time, respectively. Four spectral bands (1298.4 cm^{-1} to 1298.9 cm^{-1}, 1310.1cm^{-1} to 1312.3cm^{-1}, 1326.5 cm^{-1} to 1328 cm^{-1}, and 1331.5 cm^{-1} to 1333 cm^{-1}) in the spectral range from 1295cm^{-1} to 1335cm^{-1} were selected for the separate and simultaneous measurements of CH_4 and N_2O under normal atmospheric pressure, and all were in good agreements. The concentrations of CH_4 and N_2O of atmospheric air collected at different locations and of exhaled breath were measured and analyzed. Continuous measurements of CH_4 and N_2O concentrations of in-door laboratory air over 45 hours was also performed. It was found that raining might have effect on the N_2O concentration in out-door open-field air and anaerobic bacteria in water and soil of wetland might significantly increase the CH_4 concentration in air. The measured N_2O concentration in the central city area was somewhat lower than the reported normal level in open air. Our results demonstrated the temporal and spatial variations of CH_4 and N_2O in air.

1 Introduction

Methane (CH_4) and nitrous oxide (N_2O) are two of the most important atmospheric greenhouse gases, of which the concentrations are rising up continuously since pre-industrial time (Hartmann et al., 2013). Moreover, the global warming potential (GWP) of CH_4 is about 25 times greater than that of carbon dioxide (CO_2) (Boucher et al., 2009), while the GWP of N_2O is 300 times (Rapson and Dacres, 2014) greater than that of CO_2. Apart from natural processes, the spatial distribution of

both, to a great extent, depends on human-being activities, such as agricultural practices (Mosier et al., 1998), organic waste, industrial activities, and so on. Even small changes of concentrations of CH_4 and N_2O in atmosphere are of great influence to natural environment. Therefore, the highly sensitive and precise measurements of CH_4 and N_2O concentrations in atmospheric air are essential to environmental monitoring and greenhouse gas controlling. On the other hand, a spectral range around 7.6μm is one of the most suitable spectral bands for sensitive CH_4 and N_2O detection in air, as (1) in the wavenumber range from 1290cm^{-1} to 1350cm^{-1} CH_4 and N_2O have the second strongest fundamental vibration bands, and (2) in this spectral range there are minimum interference absorption lines from other gases (such as carbon dioxide (CO_2), carbon monoxide (CO), ammonia (NH_3), nitrogen monoxide (NO), etc.) in air except water vapor, which can be easily eliminated by drying the gas under test.

On the other hand, cavity enhanced absorption techniques, such as cavity ring-down spectroscopy (CRDS) (Banik et al., 2017), integrated cavity output spectroscopy (ICOS) (O'Keefe, 1998), noise immune cavity enhanced optical heterodyne molecular spectroscopy (NICE-OHMS) (Foltynowicz et al., 2008) and so on, have been wildly applied in sub-ppm- and even sub-ppb-level trace gas detections. The CRDS technique was first introduced by O'Keefe in 1988 (O'Keefe et al., 1988), while now many commercial instruments based on CRDS have been developed for various applications, mostly for trace gas detections and real-time monitoring. Generally, due to the use of high-fineness cavity, the equivalent absorption length of CRDS instruments is thousands to tens of thousands of times longer than that of direct absorption spectroscopy using the same-length sample cell (Romanini, 1997), therefore the measurement sensitivity of CRDS-based instruments is much improved (more than three orders of magnitude) compared to that of direct absorption spectroscopy measurements. Furthermore, compared with the traditional chemical detection methods, such as gas chromatography (GS) (Loftfield et al., 1997) and mass spectrometry (MS) (De Gouw et al., 2003), CRDS is allowed to perform real-time measurements under the premise of high-sensitivity without time-consuming sample preparations. As both high sensitivity and real-time detection are of great significance to environmental monitoring, CRDS is a suitable method for atmospheric trace gas monitoring. Moreover, CRDS also has the potential for exhaled breath test (Mashir and Dweik, 2009), since the exhaled breath contains many biomarker trace gases (for example CH_4 (De Lacy Costello *et al*., 2013), NO (Brubaker, 2016), N_2O (Bleakley and Tiedje, 1982), NH_3 (Kearney et al., 2002), etc.) that reflect some physiological processes and/or diseases in human body. However, mid-infrared (Mid-IR) CRDSs for trace gas detections were rarely reported in early days because of the unavailability of Mid-IR laser sources. Mid-IR light sources based on nonlinear optical techniques, such as quasi-phase matching difference frequency generation (QPM-DFG) (Petrov et al., 1996), had too low output power, e.g. 16 μW in (Whittaker et al., 2012), to have practical applications. In recent years, with the rapid development of advanced tunable high-power mid-infrared sources, especially external-cavity quantum cascade lasers (EC-QCL) (Botez et al., 2018), the LODs of CRDS for trace gas detections have been greatly improved. For example, Maity *et al.* (2017) achieved LOD of 52 pptv for CH_4 at 7.5 μm, Banik *et al*. (2017) achieved LOD of 5 ppbv for N_2O at 5.2 μm, Maithani *et al*. (2018) achieved LOD of 740 pptv for NH_3 at 6.3 μm and Zhou *et al*. (2018) achieved LOD of 410 pptv for NH_3 at 5.3 μm.

In this paper, we developed a trace gas sensor based on mid-infrared cw-CRDS technique with a tunable EC-MHF QCL operating at the spectral range from 1290 to 1350 cm^{-1} and applied the setup to detect trace CH_4 and N_2O in normal laboratory air and out-door atmospheric air as well as in exhaled breath. Experimentally it was observed that the measurement results were subject to a temperature fluctuation of about 0.4℃ caused by air conditioning for the laboratory room where the measurements were performed. This effect of temperature fluctuation on CRDS measurements was analysed in details and corrected via data processing, which resulted in an improvement in the measurement sensitivity of CRDS. With the correction of temperature effect, a measurement sensitivity as low as 7.38×10^{-10} cm^{-1} absorption coefficient was experimentally achieved. To achieve high measurement sensitivity as well as high reliability for separate and simultaneous detections of trace CH_4 and N_2O in atmospheric air under normal atmospheric pressure, four wavenumber bands within the spectral range of the QCL were selected for the reliable concentration determinations of CH_4 and N_2O, with one band for separate N_2O detection, two bands for separate CH_4 detection, and one band for simultaneous CH_4 and N_2O detections. The CH_4 and N_2O concentrations determined from the four bands were in good agreements, indicating the reliability of the measurement results. Finally, the developed CRDS experimental setup was used to measure the concentrations of CH_4 and N_2O collected at different locations as well as one collected exhaled breath, and to monitor simultaneously CH_4 and N_2O concentrations of in-door laboratory air continuously for over 45 hours, demonstrating the applicability of CRDS for sensitive environmental monitoring and exhaled breath analysis.

2 Experimental setup

The CRDS experimental setup is schematically depicted in Fig.1. A tunable mid-IR external-cavity CW-MHF QCL (41074-MHF, Daylight Solutions) is used as the optical source, which outputs continuously a collimated laser beam with a narrow linewidth (<10MHz) and a relatively high power (～160mW) in the spectral range from 1290cm^{-1} to 1350cm^{-1}. To block the reflection of the laser beam by the ring-down cavity optics from re-entering the QCL resonator and de-stabilizing the output spectrum and power, an optical isolator with central wavelength of 7.2 μm and isolation ratio of ＞ 30 dB (FIO-5-7.2, Innpho) is placed in front of the laser output port. Subsequently, the QCL laser beam propagates through an acousto-optic modulator (AOM, acting as a fast optical switch) (I-M041, Gooch & Housego) controlled by a home-made high-speed (with response time ＜50ns) threshold trigger, and the first-order beam outputted from the AOM is coupled into the ring-down cavity (the sample cell) consisting of a 50-cm-long stainless steel tube (CRD Optics). A pair of high-reflectivity (reflectivity > 99.98%; CRD Optics), plane concave mirrors with diameter of 1 inch and radius of curvature of -1 meter are installed at both ends of the sample cell via two three-dimensionally adjustable optical mounts. A He-Ne laser at 632.8nm is employed to help aligning the high-reflectivity cavity mirrors. The QCL laser beam that transmitted through the sample cell is focused by a focusing lens, placed closely behind the rear cavity mirror, into a highly sensitive (detectivity of 2.5×10^{9} cm√Hz/W at 8μm), TE-cooled, high-speed HgCdTe infrared photovoltaic detector (PVMI-4TE-8, Vigo, Poland). Then the detected CRD signal is recorded by a data acquisition (DAQ) card (M2i.3010, Spectrum Instrumentation, Germany) and processed by a MATLAB program in

Atmos. Meas. Tech. Discuss., https://doi.org/10.5194/amt-2018-385
Manuscript under review for journal Atmos. Meas. Tech.
Discussion started: 15 November 2018

Atmospheric Measurement Techniques Discussions

real time. As the free-spectral-range (FSR, 300MHz) of the ring-down cavity is much larger than the laser beam's linewidth, three piezoelectric transducers (PZT, Model PE-4, Thorlabs) are attached to the optical mount installing the rear high-reflectivity cavity mirror to modulate the cavity length. The PZTs are driven by a triangular wave function generated by a three-channel open-loop PZT driver (MDT694B, Thorlabs) to modulate periodically the cavity length over one half of wavelength, about 4 μm, for the coupling of QCL laser power into the ring-down cavity. Within one cavity length modulation period, laser power with a TEM_{00} mode builds up inside the ring-down cavity, correspondingly the beam power transmitted through the ring-down cavity and detected by the infrared detector also increases rapidly. At the time the detected signal amplitude exceeds a pre-set voltage threshold (20mV-2000mV), the threshold trigger sends out a triggering signal to shut down the AOM and a ring-down signal sequence is occurred and recorded by the DAQ and processed by a personal computer (PC). A vacuum pump (MPC 301Z, Welch) and a pressure gauge (LEX1, Keller) are connected to the sample cell to control the pressure of gas mixture under test and to replace gas mixture inside the sample cell when necessary.

A fitting program based on Levenberg-Marquardt algorithm is applied to fit the recorded ring-down signal to an exponential decay function to determine the ring-down time τ. By tuning the QCL wavelength, the dependence of ring-down time on wavelength over the required spectral range is obtained. The wavelength-dependent absorption coefficient α of the gas sample within the sample cell is determined from the measured ring-downtime τ using equation $\alpha(\lambda) = \frac{1}{c}\left(\frac{1}{\tau} - \frac{1}{\tau_0}\right)$, where c is the speed of light, λ is the laser wavelength, and τ_0 is the ring-down time of an "empty" cavity (without absorbing sample inside the sample cell).

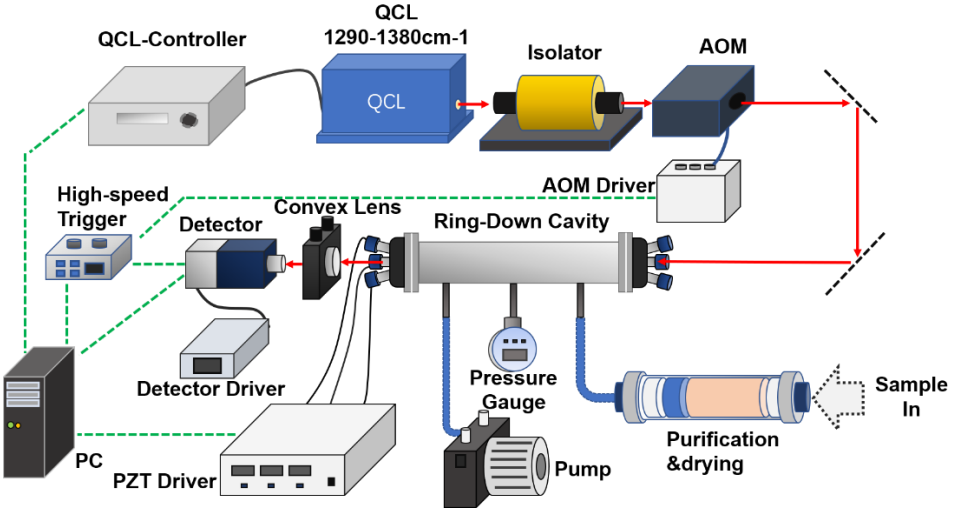

Figure 1 Schematic diagram of CRDS experimental set-up

Since in normal atmospheric air the concentration of water vapor is in the range from 100 ppm up to 4%, and water vapor has strong absorption lines in the selected spectral range from 1290cm^{-1} to 1350cm^{-1}, before measurements the water vapor in the gas mixture under test has to be mostly removed to a very low level (<1ppm) which has negligible influence on the CH_4 and

N_2O measurements. In our experiment, a 3A molecular sieve (HuShi Ltd., China), which only allows molecules whose dynamic diameter is less than 0.3 nm (Ruthven, 1984), such as water vapor and ammonia, to be adsorbed on it, is employed as the desiccants to eliminate the water vapor in the gas mixture. A filter tube, which is served as the gas inlet of the sample cell, filled up with such desiccants and quartz cotton is connected to the sample cell for purification and drying of the gas sample. In addition, a cage with the same desiccants is put inside the sample cell to absorb the water vapor leaked in, therefore to keep the sample cell nearly water vapor free. With these means for water vapor removal, this CRDS experimental setup is capable of analysing both canned dry gas mixture and untreated atmospheric air with a moderate water vapor concentration. Experimental results demonstrate the effectiveness of this drying process as no absorption lines of water vapor are observed in the measured spectra.

The gas mixtures used in the experiment are ambient air collected at different locations within the university campus in the central city area of Chengdu, China at the same period of time (3:00-5:00 p.m. June 13, 2018), three hours after a light rain. One sample is the air from the laboratory room (A), one is from an out-door parking lot outside the laboratory building (B), and one is from a wetland in the campus (C). The exhaled breath (D) of one healthy male person is also collected in the laboratory room (same as A) for measurements. In-door laboratory air is also continuously measured over 45 hours (from November 6 to 8, 2018).

3 Results and discussions

For sensitive trace gas detections, the sensitivity limit of the CRDS experimental setup is first tested with an "empty" cavity. In our case, the "empty" cavity is filled with normal laboratory air with a reduced pressure of 6.4 mbar (evacuated by the vacuum pump) and measured at an absorption-free wavenumber (1330.50 cm^{-1}). Figure 2(a) presents the recorded ring-down time of the "empty" cavity over 4400 seconds and corresponding fast Fourier transform (FFT) spectrum of the ring-down time sequence. To improve the measurement sensitivity, in general the CRDS signal is averaged to enhance the signal-to-noise ratio (SNR) of the measurements and an optimal averaging number is determined by Allan variance. Figure 3 shows the calculated Allan variance versus averaging number for the recorded "empty" ring-down time. The optimal averaging number is determined to be 151, corresponding to 21-seconds averaging time. With the optimal averaging number, the average empty ring-down time (τ_0) is 13.1 μs with a standard deviation (1σ) of 4.15×10^{-3} μs, which is translated to a minimum absorption coefficient (α_{min}) of 8.06×10^{-10} cm^{-1}. From Fig. 2(a) periodical fluctuations of the ring-down time are observed, as clearly indicated in the low-frequency end of corresponding FFT spectrum. To investigate the sources for these low-frequency periodical fluctuations, the temperature in the laboratory room is recorded simultaneously and the results are presented in Fig. 2(b). The temperature also shows periodical fluctuations with frequencies also present in the periodical fluctuations of the ring-down time, as demonstrated by the FFT spectrum of the temperature. The results presented in Fig. 2(a) and (b) clearly indicate that there is a positive correlation between the periodical fluctuations of the ring-down time and temperature in the low-

Atmos. Meas. Tech. Discuss., https://doi.org/10.5194/amt-2018-385
Manuscript under review for journal Atmos. Meas. Tech.
Discussion started: 15 November 2018

Atmospheric Measurement Techniques Discussions

frequency end. That is, the low-frequency periodical fluctuation of the measured ring-down time is partially caused by the temperature fluctuation in the laboratory room.

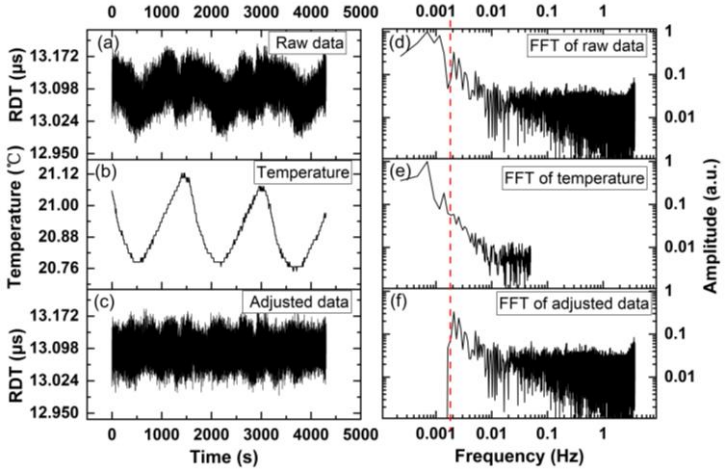

Figure 2 (a) The "empty" ring-down time sequence recorded in a long time period (over 1 hour) and (d) corresponding FFT spectrum. (b) The synchronously recorded temperature in the laboratory room and (e) corresponding FFT spectrum. (c) The "empty" ring-down time sequence after the temperature effect is eliminated and (f) corresponding FFT spectrum. RDT represents "ring-down time".

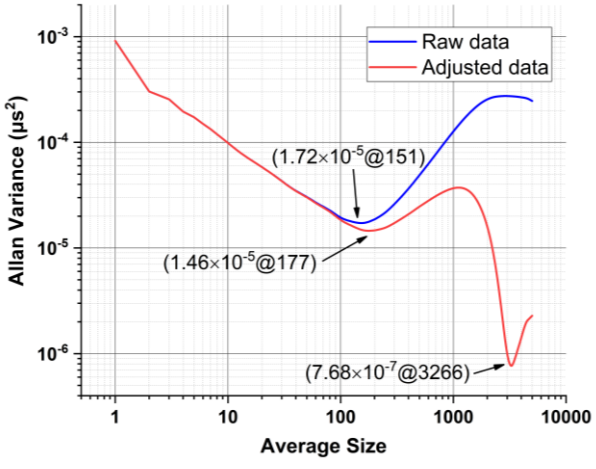

Figure 3 Allan variance plot of raw and adjusted data (without/with temperature effect correction).

A detailed investigation reveals that the correlation of ring-down time to temperature fluctuation is mainly caused by the different temperature dependence of the response of the three PZTs as well as the sensitivity of the ring-down time to the misalignment of the cavity mirrors. To test the sensitivity of the ring-down time to the alignment of the cavity mirrors, we first align the cavity mirrors to optimal positions, then apply an offset voltage to each PZT and observe how the measured ring-down time is influenced by the applied offset voltage. The results are presented in Fig. 4. An approximately linear relationship between the ring-down time and the applied offset voltage exists for each PZT, and the slopes of such linear dependences for

different PZTs are different. This phenomenon is attributed to the PZT's difference in the creep and thermal-drift characteristics. As normally known, PZT is a nonlinear component and no two PZTs' characteristics are identical (Jaffe et al., 1971). Moreover, in our experiment the PZTs are controlled in an open-loop mode. Due to the different temperature sensitivity of the response of each PZT, temperature fluctuation causes mis-alignment of the cavity mirrors, which further results in a fluctuation in measured ring-down time, as presented in Fig. 2(a). Other thermal effects, such as the cavity length fluctuation, reflectivity fluctuation caused by temperature fluctuation, are negligible as compared to cavity alignment fluctuation.

To eliminate the effect of temperature fluctuation on trace gas detection with CRDS, those frequency points in the FFT spectrum of ring-down time also presented in the FFT spectrum of the temperature fluctuation (the low-frequency end in our case) are filtered out mathematically and the ring-down time sequence is adjusted accordingly, as presented in Fig. 2(c). After the effect of temperature fluctuation on the ring-down time measurement is eliminated, the absorption coefficient sensitivity limit α_{min} is first improved to 7.38×10^{-10} cm^{-1}, with the optimal averaging number changes to 177, corresponding to 26.4 seconds averaging time, as presented in Fig. 3. Figure 3 also shows that there is a second minimum Allan variance if the averaging time is further increased, indicating α_{min} can be further improved to 1.70×10^{-10} cm^{-1} with optimal averaging number of 3266 and corresponding averaging time of 490 seconds. The results demonstrate that with temperature effect correction the measurement sensitivity could be greatly improved with a compromise of increasing measurement time (490 seconds versus 21 seconds).

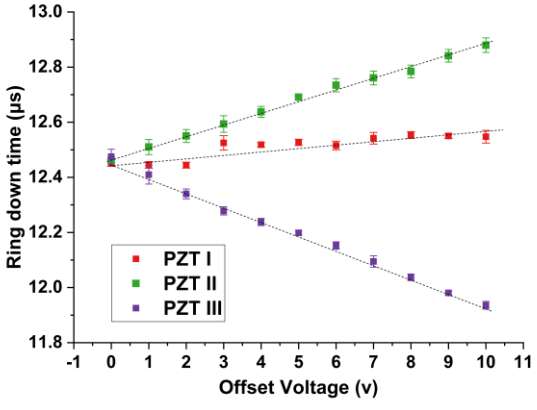

Figure 4 Linear relationship between the offset voltage on each PZTs and the measured ring-down time.

For real trace gas detections, the sensitivity limit achieved above with the "empty" cavity may not be fulfilled due to the presence of absorbing sample in the cavity and other effects such as laser wavelength fluctuation, limited wavelength tuning step for spectral measurement, etc. To find out the limits of detection (LOD) of CH_4 and N_2O with the CRDS experimental setup, the sample cell is filled with ambient air at 1 atmospheric pressure and the ring-down data is recorded continuously at peaks of the absorption lines of CH_4 (1298.60 cm^{-1}) and N_2O (1327.07 cm^{-1}), respectively, and the corresponding Allan variances are calculated. The achieved minimum σ_{Allan} values are 3.12×10^{-9} cm^{-1} at 1327.07 cm^{-1} for CH_4, and 2.75×10^{-9} cm^{-1}

at 1298.60cm^{-1} for N_2O, which correspond to an LOD of 22.3 pptv for CH_4 and 15.5 pptv for N_2O, respectively. These LODs are obtained with approximate 15-seconds averaging time. The achieved LODs are lower than that achieved by other groups employing CRDS for CH_4 and N_2O detections in recent years, as described in Sec. 1.

The LODs for CH_4 and N_2O detections can be improved by eliminating the effect of temperature fluctuation via the process presented above. Again two Allan variance minima are present in the dependence of Allan variance on averaging time after the temperature effect is corrected, the corresponding LODs for CH_4 and N_2O detections are 18.2 pptv and 14.9 pptv with 24.9-seconds and 20.5-seconds averaging time for the first minimum, and 3.62 pptv and 4.67 pptv with 513-seconds and 461-seconds averaging time for the second minimum, respectively. Such low LODs allow sensitive detections of CH_4 and N_2O with sub-ppbv-level concentrations.

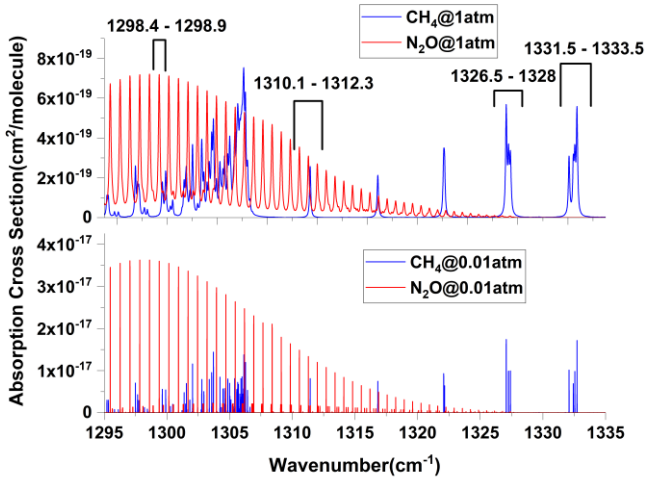

Figure 5 HITRAN spectra of N_2O and CH_4 in the spectral range from 1295 cm^{-1} to 1335 cm^{-1}, at (a) one atmospheric pressure and (b) 0.01 atmospheric pressure, respectively.

For simultaneous detections of CH_4 and N_2O in real applications, the optimal absorption lines or spectral ranges have to be carefully selected. For the spectral range from 1290cm^{-1} to 1350cm^{-1}, N_2O and CH_4 both have strong absorption lines. Figure 5 shows the spectral lines of N_2O and CH_4 in the spectral range from 1295cm^{-1} to 1335cm^{-1} at 1 and 0.01 atmospheric pressures, respectively (The spectral data are from HITRAN 2016). When the pressure in the sample cell is reduced, individual absorption lines are well separated and can be fitted independently. At 1 atmospheric pressure, on the other hand, absorption lines are mixed and partially overlapped, especially when CH_4 and N_2O are both presented. In this case care has to be taken to select appropriate spectral band(s) for separate or simultaneous detections of CH_4 and N_2O. In our experiment, four spectral sections in the spectral range from 1295cm^{-1} to 1335cm^{-1} are tested for the detections of CH_4 and N_2O. That is, Section A: from 1298.4 cm^{-1} to 1298.9 cm^{-1}, contains one N_2O absorption line (wavenumber 1298.6031 cm^{-1}, line strength 1.681×10^{-19} cm^{-1}/(molec·cm^{-2})), which is slightly weaker than the strongest N_2O absorption line (1297.8315 cm^{-1}, 1.689×10^{-19} cm^{-1}/(molec·cm^{-2}) but is well separated from the adjacent absorption lines of CH_4 and N_2O. Section B: from 1310.1cm^{-1} to 1312.3cm^{-1}, in which there are

Atmos. Meas. Tech. Discuss., https://doi.org/10.5194/amt-2018-385
Manuscript under review for journal Atmos. Meas. Tech.
Discussion started: 15 November 2018

Atmospheric Measurement Techniques Discussions

three N_2O lines and one CH_4 line. These four absorption lines are sufficiently strong and well separated. Sections C (from 1326.5 cm^{-1} to 1328 cm^{-1}) and D (from 1331.5 cm^{-1} to 1333 cm^{-1}) contain two strong absorption lines of CH_4 which are well separated from the absorption lines of N_2O in the measurable spectral range, with each line is the combination of several overlapped lines. Therefore, Section A is used for independent N_2O detection, while Sections C and D are used for independent CH_4 detection, and Section B is for simultaneous CH_4 and N_2O detections.

Figure 6 shows the measured spectral lines and corresponding best fits for the ambient air collected in the laboratory room. The measured data are the average of 128 measurements, took approximate 5 seconds for each wavenumber point. From Section A, the N_2O concentration is determined to be 0.224±0.002ppmv. From Sections C and D, the CH_4 concentration is determined to be 1.698±0.002ppmv and 1.697±0.002ppmv, respectively, while from Section B, the CH_4 and N_2O concentrations are determined to be 1.700±0.002ppmv and 0.222±0.002ppmv, respectively. The small differences among the concentration values determined from different sections are mainly due to the misalignment caused by AOM induced small change in the deflection angle of the diffracting laser beam when tuning the laser wavenumber. Overall the CH_4 and N_2O concentrations determined from different sections are well consistent, indicating the reliability of the measurement results. The good agreements between the CH_4 and N_2O concentrations determined separately (from sections A, C, and D) and simultaneously (from section B) demonstrate that CH_4 and N_2O concentrations can be simultaneously determined by employing a narrow band containing absorption lines of both gases for spectral measurements, therefore to shorten the measurement time.

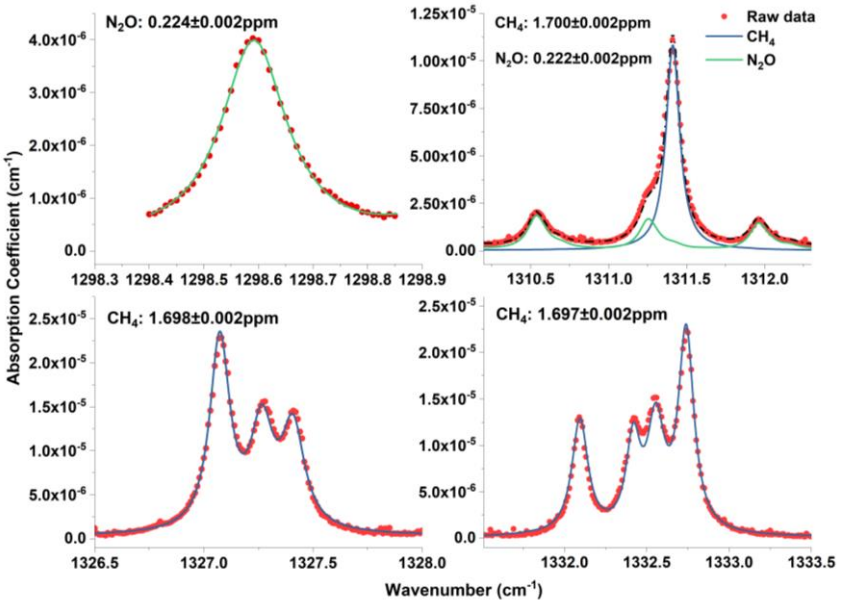

Figure 6 Measured spectra (circles) and corresponding best fits (solid lines) for four selected spectral bands (A: 1298.3-1299.1 cm^{-1}, B: 1310.1-1312.3 cm^{-1}, C: 1326.5-1328 cm^{-1}, and D: 1331.5-1333.5 cm^{-1}).

Atmos. Meas. Tech. Discuss., https://doi.org/10.5194/amt-2018-385
Manuscript under review for journal Atmos. Meas. Tech.
Discussion started: 15 November 2018

Atmospheric Measurement Techniques Discussions

It is worth mentioning that for the measurements presented in Fig. 6, the effect of temperature fluctuation is not eliminated due to the relatively high concentration values compared to the LODs as well as relatively short measurement time. Still, the temperature fluctuation caused uncertainty of CH_4 and N_2O concentration is presented in the determined concentration values, though this uncertainty is small and can be neglected in our case, can be corrected if necessary.

The CRDS experimental setup is then used to measure the CH_4 and N_2O concentrations in ambient air collected at different locations and in exhaled breath of one healthy person under 1 atmospheric pressure. The results are presented in Fig. 7 and show that, (1) the N_2O concentration in the in-door air of laboratory room is higher than that of out-door open fields (parking lot and wetland) (0.206 ppmv versus 0.135-0.137 ppmv). This phenomenon might be due to the effect of raining before the sample gas collection on the N_2O concentration of out-door air. (2) The CH_4 concentration of out-door air collected at wetland is higher than that collected at parking lot (3.184 ppmv versus 2.002 ppmv), while the N_2O concentration is little changed (0.135 ppmv versus 0.137 ppmv). This observation might be attributed to the release of CH_4 from the anaerobic bacteria in water and soil of wetland (Cao et al., 1998). (3) The CH_4 concentration of exhaled breath is approximately 169 ppbv higher than the environmental air (2.204 ppmv versus 2.035 ppmv in the laboratory room), while the change in N_2O concentration is not significant (0.205 ppmv versus 0.206 ppmv). The slight variance in CH_4 concentration demonstrates the physiological process of CH_4 in human body. The concentration of CH_4 is closely related to some anaerobic fermentations, such as M. smithii, in human gut (Kim et al., 2012). From these measurements it is found that the measured N_2O concentration of air samples, which is between 0.206 ppmv and 0.135 ppmv, is lower than the reported normal level of open air, about 0.3ppm (Davidson, 2009). This might be due to the air samples measured in our experiment are collected in a central city area, which is far away from agricultural areas where N_2O is mainly produced via agricultural practices.

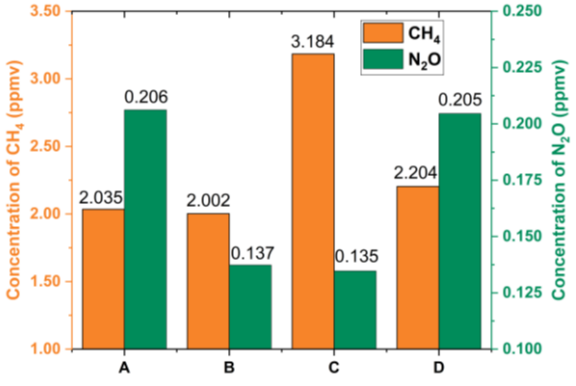

Figure 7 Measured CH_4 and N_2O concentrations in ambient air collected at different locations (A, B, C) and in exhaled breath (D). A: Laboratory room, B: Parking lot, C: Wetland, D: Exhaled breath of one healthy person collected at the laboratory room.

Finally, the experimental setup is used to measured continuously the concentrations of CH_4 and N_2O of laboratory air for 45.5 hours from 17:00PM November 6 to 14:30PM November 8, 2018. The results are presented in Fig. 8. The laboratory air is continuously flowing into/out the sample cell at a flow rate of approximately 2 L/min at normal atmospheric pressure. The

Atmos. Meas. Tech. Discuss., https://doi.org/10.5194/amt-2018-385
Manuscript under review for journal Atmos. Meas. Tech.
Discussion started: 15 November 2018

Atmospheric Measurement Techniques Discussions

measurements are performed with the spectral band B from 1310.1cm^{-1} to 1311.8cm^{-1}. Slow fluctuations of CH_4 and N_2O concentrations are observed due to regular air exchange (controlled by an air conditioner) between in-door laboratory air and out-door open air. In the meantime, a fast fluctuation of N_2O concentration is also observed which is well above the measurement uncertainty and not presented in the measured CH_4 concentration. The reason(s) for this fast N_2O fluctuation is unknown, probably due to the operations of air conditioner specified for the laboratory room and of other air conditioners (close to the air exchange point) for the whole building. It is noticed that the measured N_2O concentrations are higher than that measured on June 13, 2018 and are within the reported normal range of open air, while the measured CH4 concentrations are comparable to that measured on June 13.

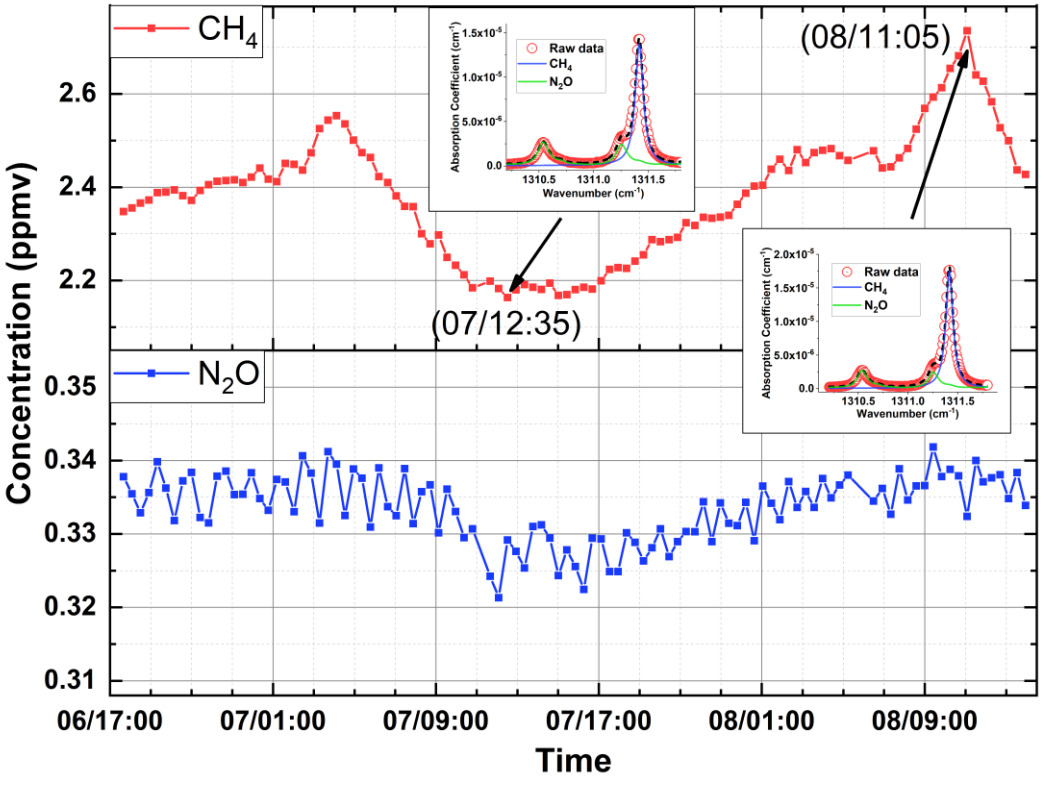

Figure 8 Measured CH_4 and N_2O concentrations in laboratory room (Location A) for a period of 45.5 hours from 17:00PM November 6 to 14:30PM November 8, 2018. Insets are the measured absorption spectra at two different time series and corresponding best fits for the determination of CH_4 and N_2O concentrations.

It is worth mentioning that in the measurement results presented in Figs. 7 and 8, the effect of temperature fluctuation is not eliminated, as the measurement sensitivity of CRDS experimental setup without temperature effect correction is sufficiently high that makes the correction un-necessary. Still, the idea to eliminate the effect of temperature fluctuation on the trace gas detection presented in this paper is helpful to situations where very high sensitivity is required for the detection of trace gases in locations where temperature is not well controlled, for example, long-term unattended out-door or wild-field monitoring of

trace gases in the ppbv to sub-ppbv levels. In open fields the temperature changes widely during day and night and the effect of temperature fluctuation may become significant. The temperature effect can be eliminated by measuring the temperature dependence of measured concentrations before the CRDS instruments are placed to the wild fields. Once the CRDS instruments are in place where temperature is monitored, the temperature effect can be corrected accordingly.

4 Conclusion

We have developed an ultra-highly sensitive trace gas sensor based on mid-infrared cw-CRDS technique, in which a tunable EC-QCL at central wavelength of ~7.6 μm was employed to cover several strong absorption lines of CH_4 and N_2O. We have observed low-frequency periodical fluctuations of measured ring-down time, and correlated ring-down time fluctuations mainly to temperature fluctuations presented in test site. It was found that such correlation was attributed to creep and thermal-drift characteristics of PZTs employed to modulate the cavity length for coupling the laser power into the ring-down cavity. By mathematically eliminating the effect of temperature fluctuation, a sensitivity limit of 7.38×10^{-10} cm^{-1} has been experimentally achieved with 26.4-seconds averaging time and could be further improved to 1.70×10^{-10} cm^{-1} with 490-seconds averaging time. For CH_4 and N_2O absorption lines located at 1298.60 cm^{-1} and 1327.07 cm^{-1}, with temperature effect correction detection limits of 18.2 pptv and 14.9 pptv were experimentally achieved with 24.9-seconds and 20.5-seconds averaging time, and could be further improved to 3.62 pptv and 4.67 pptv by increasing the averaging time to 513 seconds and 461 seconds, respectively. The measurements of CH_4 and N_2O concentrations with different spectral bands have demonstrated that CH_4 and N_2O concentrations could be simultaneously determined at one atmospheric pressure with high precision. Finally, this CRDS setup could be easily adapted for the detections of other gases such as C_2H_2, H_2O_2, H_2S, SO_2 and sulfides with anticipated detection limits in the ppbv or even pptv level.

Data availability. Data are available from the authors upon request.

Author contribution. BL and JT designed the experiments and JT and JW performed the experiments and data processing. JT and BL prepared the manuscript with contributions from all co-authors.

Competing interests. The authors declare that they have no conflict of interest.

References

Banik, G. D., Som, S., Maity, A., Pal, M., Maithani, S., Mandal, S. and Pradhan, M.: An EC-QCL based N2O sensor at 5.2 μm using cavity ring-down spectroscopy for environmental applications, Anal. Methods, 9(15), 2315–2320, doi:10.1039/c7ay00482f, 2017.

Bleakley, B. H. and Tiedje, J. M.: Nitrous-Oxide Production By Organisms Other Than Nitrifiers or Denitrifiers, Appl. Environ. Microbiol., 44(6), 1342–1348, 1982.

Botez, D., Kirch, J. D., Boyle, C., Oresick, K. M., Sigler, C., Kim, H., Knipfer, B. B., Ryu, J. H., Lindberg, D., Earles, T., Mawst, L. J. and Flores, Y. V: High-efficiency, high-power mid-infrared quantum cascade lasers [Invited], Opt. Mater. Express, 8(5), 1378–1398, doi:10.1364/OME.8.001378, 2018.

Boucher, O., Friedlingstein, P., Collins, B. and Shine, K. P.: The indirect global warming potential and global temperature change potential due to methane oxidation, Environ. Res. Lett., 4(4), doi:10.1088/1748-9326/4/4/044007, 2009.

Brubaker, P. H.: Use of Exhaled Nitric Oxide Measurements to Guide Treatment in Chronic Asthma, J. Cardiopulm. Rehabil. Prev., 36(2), 140–141, doi:10.1097/HCR.0000000000000175, 2016.

Cao, M., Gregson, K. and Marshall, S.: Global methane emission from wetlands and its sensitivity to climate change, Atmos. Environ., 32(19), 3293–3299, doi:10.1016/S1352-2310(98)00105-8, 1998.

Davidson, E. A.: The contribution of manure and fertilizer nitrogen to atmospheric nitrous oxide since 1860, Nat. Geosci., 2, 659 [online] Available from: http://dx.doi.org/10.1038/ngeo608, 2009.

Foltynowicz, A., Schmidt, F. M., Ma, W. and Axner, O.: Noise-immune cavity-enhanced optical heterodyne molecular spectroscopy: Current status and future potential, Appl. Phys. B Lasers Opt., 92(3 SPECIAL ISSUE), 313–326, doi:10.1007/s00340-008-3126-z, 2008.

De Gouw, J., Warneke, C., Karl, T., Eerdekens, G., Van der Veen, C. and Fall, R.: Sensitivity and specificity of atmospheric trace gas detection by proton-transfer-reaction mass spectrometry, Int. J. Mass Spectrom., 223–224, 365–382, doi:10.1016/S1387-3806(02)00926-0, 2003.

Hartmann, D. L., Tank, A. M. G. K., Rusticucci, M., Alexander, L. V, Brönnimann, S., Charabi, Y. A. R., Dentener, F. J., Dlugokencky, E. J., Easterling, D. R. and Kaplan, A.: Observations: atmosphere and surface, in Climate Change 2013 the Physical Science Basis: Working Group I Contribution to the Fifth Assessment Report of the Intergovernmental Panel on Climate Change, Cambridge University Press., 2013.

Jaffe, B., Cook, W. R. and Jaffe, H.: Piezoelectric ceramics., Elsevier., 1971.

Kearney, D. J., Hubbard, T. and Putnam, D.: Breath ammonia measurement in Helicobacter pylori infection, Dig. Dis. Sci., 47(11), 2523–2530, doi:10.1023/A:1020568227868, 2002.

Kim, G., Deepinder, F., Morales, W., Hwang, L., Weitsman, S., Chang, C., Gunsalus, R. and Pimentel, M.: Methanobrevibacter smithii is the predominant methanogen in patients with constipation-predominant IBS and methane on breath, Dig. Dis. Sci., 57(12), 3213–3218, doi:10.1007/s10620-012-2197-1, 2012.

De Lacy Costello, B. P. J., Ledochowski, M. and Ratcliffe, N. M.: The importance of methane breath testing: A review, J. Breath Res., 7(2), doi:10.1088/1752-7155/7/2/024001, 2013.

Loftfield, N., Flessa, H., Augustin, J. and Beese, F.: Automated Gas Chromatographic System for Rapid Analysis of the Atmospheric Trace Gases Methane, Carbon Dioxide, and Nitrous Oxide, J. Environ. Qual., 26(2), 560, doi:10.2134/jeq1997.00472425002600020030x, 1997.

Maithani, S., Mandal, S., Maity, A., Pal, M. and Pradhan, M.: High-resolution spectral analysis of ammonia near 6.2 μm using a cw EC-QCL coupled with cavity ring-down spectroscopy, Analyst, 143(9), 2109–2114, doi:10.1039/C7AN02008B, 2018.

Maity, A., Pal, M., Banik, G. D., Maithani, S. and Pradhan, M.: Cavity ring-down spectroscopy using an EC-QCL operating at 7.5 μm for direct monitoring of methane isotopes in air, Laser Phys. Lett., 14(11), doi:10.1088/1612-202X/aa8584, 2017.

Mashir, A. and Dweik, R. A.: Exhaled breath analysis: The new interface between medicine and engineering, Adv. Powder Technol., 20(5), 420–425, doi:10.1016/j.apt.2009.05.003, 2009.

Mosier, A. R., Kroeze, C., Nevison, C., Oenema, O. and Seitzinger, S.: Closing the global N 2 O budget : nitrous oxide emissions through the agricultural nitrogen cycle inventory methodology, Nutr. Cycl. Agroecosystems, 52(2–3), 225–248, doi:10.1023/A:1009740530221, 1998.

O'Keefe, a, Deacon, D. a G. and Okeefe, a: Cavity Ring-Down Optical Spectrometer for Absorption measurements using pulsed laser sources, Rev. Sci. Instrum., 59(12), 2544, doi:10.1063/1.1139895, 1988.

O'Keefe, A.: Integrated cavity output analysis of ultra-weak absorption, Chem. Phys. Lett., 293(5–6), 331–336, doi:10.1016/S0009-2614(98)00785-4, 1998.

Petrov, K. P., Goldberg, L., Burns, W. K., Curl, R. F. and Tittel, F. K.: Detection of CO in air by diode-pumped 4.6-microm difference-frequency generation in quasi-phase-matched LiNbO(3)., Opt. Lett., 21(1), 86–8, doi:10.1364/ol.21.000086, 1996.

Rapson, T. D. and Dacres, H.: Analytical techniques for measuring nitrous oxide, TrAC - Trends Anal. Chem., 54, 65–74, doi:10.1016/j.trac.2013.11.004, 2014.

Romanini, D.: CW cavity ring down spectroscopy, Chem. Phys. Lett., 264(3–4), 316–322, doi:10.1016/S0009-2614(96)01351-6, 1997.

Ruthven, D. M.: Principles of adsorption and adsorption processes, John Wiley & Sons., 1984.

Whittaker, K. E., Ciaffoni, L., Hancock, G., Peverall, R. and Ritchie, G. A. D.: A DFG-based cavity ring-down spectrometer for trace gas sensing in the mid-infrared, Appl. Phys. B Lasers Opt., 109(2), 333–343, doi:10.1007/s00340-012-5150-2, 2012.

Zhou, S., Han, Y. and Li, B.: Pressure optimization of an EC-QCL based cavity ring-down spectroscopy instrument for exhaled NO detection, Appl. Phys. B Lasers Opt., 124(2), 1–8, doi:10.1007/s00340-018-6898-9, 2018.